JOC The Journal of Organic Chemistry

Article

pubs.acs.org/joc

Amine Superbases Stabilized by Extended Hydrogen Bond Networks

Steven M. Bachrach*

Department of Chemistry, Trinity University, 1 Trinity Place, San Antonio, Texas 78212, United States

Supporting Information

ABSTRACT: Extended hydrogen-bonding networks as a mechanism for creating superbases is explored through six different amine scaffolds: linear acenes, cyclohexane, decalin, triptycene, adamantane, and [2.2]paracyclophane. The gas-phase proton affinities of 21 different potential superbases were computed at the ωB97X-D/6-311+G(2d,p) level. This method was benchmarked against the experimental proton affinities of 44 nitrogen bases. Extended hydrogen-bonding networks, including second- and third-layer hydrogen bonding, led to bases with proton affinities 20 kcal mol^{-1} greater than that of bis(dimethylamino)naphthalene. The strongest bases are the decalin base **25** and the adamantane base **31**.

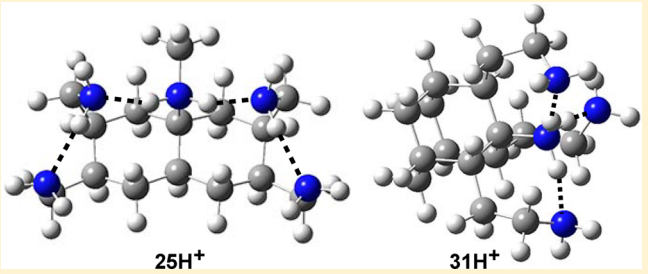

INTRODUCTION

The quest for strong organic bases began with the development of 1,8-bis(dimethylamino)naphthalene (**1**, DMAN), also known as proton sponge.[1] Compounds with basicities greater than that of DMAN have been christened superbases. Superbases often involve some degree of intramolecular hydrogen bonding to stabilize the resulting conjugate acid. Many superbases rely on placing two or more amino groups in near proximity.[2−6] Other variations involve use of phosphazenyl[7−9] or guanidinyl[10−12] groups or supermolecular pyridinyl[13,14] scaffolds. Computational approaches have provided useful guidance toward the development of new superbases. The review by Maksić, Kovačević, and Vianello details the development of many families of superbases.[15]

Our first foray into the field of superbases proposed pyridine and quinuclidine scaffolds[16] possessing remote groups with lone pairs that could move to form hydrogen bonds to a protonated nitrogen. The two best examples we discovered are **2** and **3**.

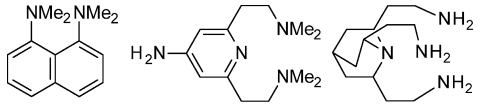

1 **2** **3**

Given the fact that superbases often rely on intramolecular hydrogen bonding[15] to stabilize the conjugate acid, Kass speculated that a *network* of hydrogen bonding might afford even more stabilization of the conjugate acid, creating even more powerful superbases.[17] The tetraamine **4**, when protonated at the central amine, can form three intramolecular hydrogen bonds in its conjugate acid **4H**$^+$. The experimental gas-phase proton affinity (PA) of **4** is 256.2 kcal mol^{-1}; the B3LYP/aug-cc-pVDZ method estimates its value as 261.3 kcal mol^{-1}. The heptaamine **5** can provide a second layer of hydrogen bonding—beginning a hydrogen-bonding network—in its conjugate acid **5H**$^+$; the estimated PA (B3LYP/aug-cc-pVDZ) of **5** is 288.5 kcal mol^{-1}, for an increase in the PA of over 27 kcal mol^{-1} afforded by the second layer of hydrogen bonding. Kass has also applied this concept toward creating strong acids.[18−20] Remote hydroxyl groups in polyols form extended hydrogen-bonding networks that result in very acidic alcohols.

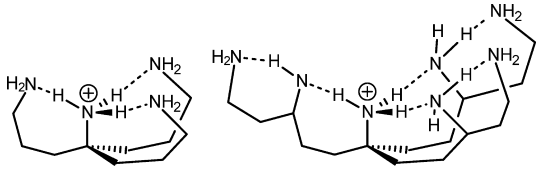

4H$^+$ **5H**$^+$

We report here a computational study of a number of different superbase scaffolds that allow for a hydrogen-bonding network. The scaffolds include linear acenes, cyclohexane, decalin, triptycene, adamantane, and [2.2]paracyclophane. This study extends our earlier communication of results pertaining to the linear acene scaffold.[21]

RESULTS AND DISCUSSION

Benchmarking of Amine Basicity. In order to assess the computational method, we computed the gas-phase PAs of 44 simple nitrogen bases. The experimental values for the gas-phase PAs of these compounds were obtained from the NIST Webbook database.[22] This set spans a range of proton affinities of over 80 kcal mol^{-1}, from hydrogen cyanide (PA = 170.4 kcal mol^{-1}) to DBU (PA = 250.45 kcal mol^{-1}). It is important to note that the gas-phase PAs of the strong bases DMAN and DBU have been reported and are included in this set. The

Received: August 27, 2013
Published: October 4, 2013

   dx.doi.org/10.1021/jo4018974 | J. Org. Chem. 2013, 78, 10909−10916

values of the differences between the computed PAs [ΔH^{298} using the 6-311+G(2d,p) basis set and the B3LYP,[23] M06-2X,[24] and ωB97X-D[25] functionals] and the experimental values are listed in Table 1.

Table 1. Comparison of Experimental[a] Proton Affinities (ΔH^{298}, kcal mol^{-1}) of Simple Nitrogen Bases and Their Differences with Values Computed[b] Using Various Density Functionals

		difference		
base	exptl[a]	B3LYP	M06-2X	ωB97X-D
hydrogen cyanide	170.4	2.80	4.78	0.44
propanedinitrile	172.8	0.79	3.74	−0.95
4-nitrobenzonitrile	185.4	−0.34	4.20	−1.19
acetonitrile	186.2	−0.12	2.76	−2.04
propanenitrile	189.8	0.13	3.22	−1.63
isobutylnitrile	192.1	−0.19	3.11	−1.75
benzonitrile	194.0	−2.29	2.32	−2.95
cyclohexanenitrile	194.8	−1.24	2.43	−2.45
1,3,5-triazine	202.9	3.03	5.82	0.93
hydrazine	203.9	−0.36	1.03	−3.01
ammonia	204.0	2.28	3.49	−0.53
pyrazine	209.6	1.11	4.30	−0.77
aniline	210.9	2.44	3.47	0.06
1*H*-pyrazole	213.7	0.70	3.68	−1.50
methylamine	214.9	2.04	3.33	−0.57
aziridine	216.4	0.84	2.99	−1.66
pyridazine	216.8	−1.07	1.92	−3.26
ethylamine	218.0	1.59	2.77	−0.90
isopropylamine	220.8	1.63	3.11	−0.88
pyridine	222.0	0.21	3.34	−1.87
dimethylamine	222.2	2.34	3.71	−0.30
cyclohexanamine (**14**)	223.3	1.07	2.71	−1.31
1,8-naphthalenediamine (**6**)	225.7	2.03	4.49	−0.41
pyrrolidine	226.6	0.91	2.41	−2.12
1,1,2,2-tetramethylhydrazine	226.7	2.94	4.07	0.27
trimethylamine	226.8	2.68	3.52	−0.27
adamantan-1-amine	226.8	0.74	2.35	−1.60
1,2-ethanediamine	227.4	2.10	3.93	−0.62
piperidine	228.0	1.59	2.86	−1.07
DABCO	230.3	0.79	2.24	−1.84
N-methylpyrrolidine	230.8	2.66	3.70	−0.13
N-methylpiperidine	232.1	2.18	3.15	−0.70
diisopropylamine	232.3	1.61	3.06	−0.99
4-aminopyridine	234.2	−0.78	2.53	−2.79
triethylamine	234.7	1.98	2.96	−0.85
quinuclidine	235.0	1.78	2.44	−1.14
guanidine	235.7	0.06	2.55	−2.93
1,3-propanediamine	235.9	2.09	4.05	−0.27
4-dimethylaminopyridine	238.4	−1.67	1.77	−3.37
1,4-butanediamine	240.3	1.26	2.58	−1.26
N,*N*,*N*′,*N*′-tetramethyl-1,2-ethanediamine	242.07	3.63	5.78	1.13
DMAN (**1**)	245.75	1.13	4.69	−1.92
N,*N*,*N*′,*N*′-tetramethyl-1,4-butanediamine	250.07	4.45	5.16	0.53
DBU	250.45	−0.41	2.00	−3.08
mean difference		1.16	3.29	−1.22
mean unsigned difference		1.55	3.28	1.37
maximum difference		4.45	5.82	3.37

[a]From ref 22. [b]All computations used the 6-311+G(2d,p) basis set.

While B3LYP/6-311+G(2d,p) affords the smallest *mean* difference with the experimental PA values, the other statistical measures point toward ωB97X-D as the superior choice. With this functional, the mean unsigned difference is the smallest (1.37 kcal mol^{-1} vs 1.55 kcal mol^{-1} for B3LYP and 3.28 kcal mol^{-1} for M06-2X). The largest error when using ωB97X-D is 3.37 kcal mol^{-1} (4-dimethylaminopyridine), while the largest error is more than 1 kcal mol^{-1} greater with B3LYP and 2.5 kcal mol^{-1} greater with M06-2X.

The plot relating the ωB97X-D-calculated PAs with the experimental values is shown in Figure 1. The least-squares fit

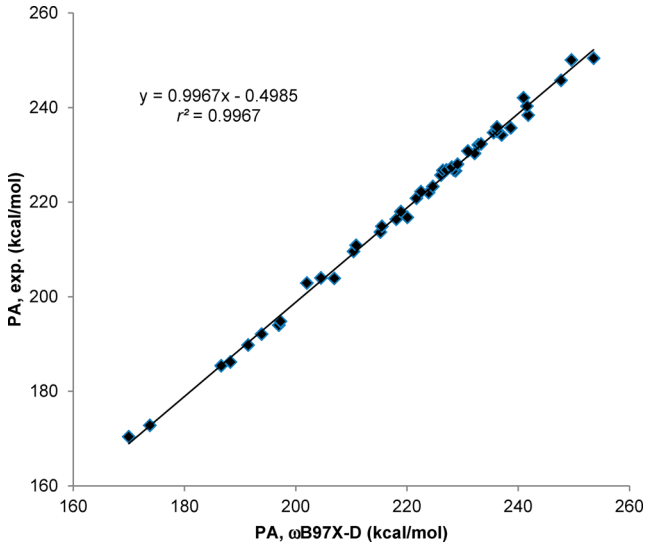

Figure 1. Comparison of the ωB97X-D-calculated proton affinities to the experimental proton affinities.

line relating these data has a slope near unity and an intercept quite close to zero, with r^2 = 0.9967. One can therefore use the ωB97X-D-computed PA values without correction. However, the relationship between the experimental PA values and those computed with the other two methods is not as good (see Figures S1 and S2 in the Supporting Information). Though the correlation coefficients are also quite close to 1, their intercepts are significantly different from zero, and so some correction would be mandatory with their usage.

The relatively poor performance of M06-2X is somewhat surprising given the strong reputation of this functional. On the other hand, the performance of B3LYP is perhaps better than expected given the recent rash of negative comments about this functional.[26−29] We opted to employ the ωB97X-D/6-311+G(2d,p) method for the study of the superbases reported here, and we report PA values without any further corrections.

Computational Method. The gas-phase geometries of all of the bases and their conjugate acids were optimized at the ωB97X-D/6-311+G(2d,p) level. Multiple conformations were examined for each base and its conjugate acid. This entailed exploring conformations resulting from rotations about C−C and C−N single bonds where appropriate, along with differing arrangements of the hydrogen-bonding network (i.e., swapping which groups are hydrogen-bond donors and acceptors). Analytical frequencies were computed to confirm that all structures were local energy minima. The frequencies were used without scaling to compute zero-point vibrational energies and enthalpies (evaluated at 298.15 K). We report here all of the

dx.doi.org/10.1021/jo4018974 | J. Org. Chem. 2013, 78, 10909−10916

PAs as ΔH^{298} values. All of the computations were performed with the Gaussian 09 suite.[30]

Linear Acene Bases. The linear acene bases were discussed in a previous paper.[21] The highlights of that work are summarized here.

Since the reference superbase DMAN (**1**) has amino groups positioned in a 1,8 relationship on naphthalene, the natural extension is to the anthracene analogue **7** with amino groups at the 1, 8, and 9 positions. This can be further extended to the tetracene analogue **8**. The series **6**, **7**, and **8** tests the role of adding an additional first-layer hydrogen bond (a hydrogen bond to the quaternary amine) and a second-layer hydrogen bond within the conjugate acid. These hydrogen bonds are indicated in Scheme 1. Their computed PAs are listed in Table 2.

Scheme 1

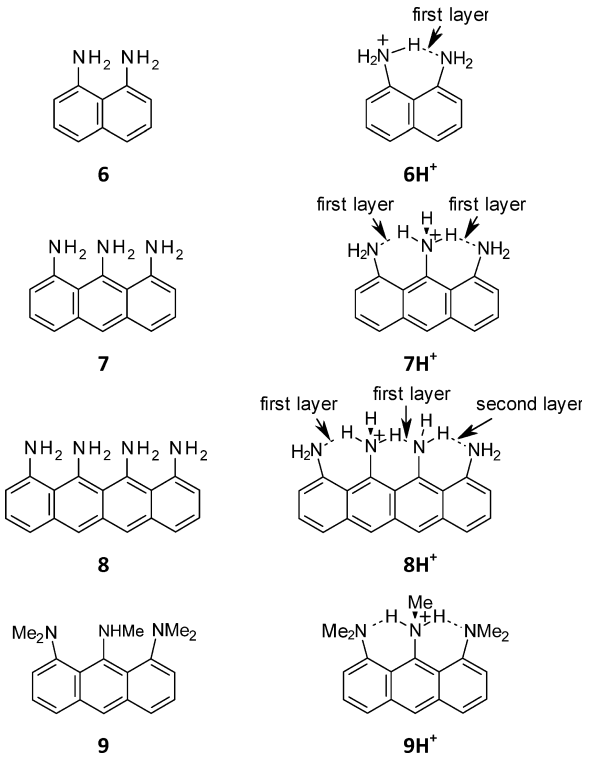

Table 2. ωB97X-D/6-311+G(2d,p)-Computed Proton Affinities (kcal mol^{-1}) of 6−13 and PAs Relative to That of 1

compound	PA	rel. PA
1	247.7	0.0
6	226.1	−21.6
7	232.7	−15.0
8	234.5	−13.2
9	251.8	4.1
10	246.4	−1.3
11	257.3	9.6
12	261.1	13.4
13	262.2	14.5

The first issue to address is that compounds **6**−**8** are much less basic than **1**. This is due to two reasons. First, the methyl groups on the amine of **1** stabilize the positive charge of the conjugate acid **1H**$^+$, making the compound more basic. Second, in the primary amines **6**−**8**, hydrogen bonding occurs between the amine groups, stabilizing the free amine. However, the methyl groups of **1** eliminate the intramolecular hydrogen bonds and provide some steric repulsion between the dimethylamino groups, destabilizing the free amine. These two effects combine to make tertiary amine **1** much more basic than the primary amines **6**−**8**.

The effect of the methyl groups can be seen with **9**. Here the methyl group on the central amine can stabilize the positive charge in the conjugate acid, and the methyl groups on the terminal amines minimize the intramolecular hydrogen bonding and provide some steric destabilization of the free base. The net result is that the PA of **9** is 19.1 kcal mol^{-1} greater than that of **7** and 4.1 kcal mol^{-1} greater than that of **1**.

The PA increases in the series **6** to **7** to **8**, supporting the notion of increased basicity with increasing hydrogen bonding, including hydrogen bonding in the second layer. However, the increase afforded by the second-layer hydrogen bond here is small, as indicated by only a 1.8 kcal mol^{-1} increase in the PA of **8** over **7**.

Hydrogen bonds are of maximum strength when the X−H···Y angle is 180°. The angles of the hydrogen bonds in **7**−**9** are not ideal; the N−H···H angles in **7H**$^+$ and **9H**$^+$ are 142.8° and 145.2°, respectively, while the three N−H···H angles in **8H**$^+$ are 142.7°, 141.2°, and 138.2°. What is needed is for the amino groups to be positioned not in a 1,3-arrangement but farther apart. The 1,4-arrangement in **10** allows the formation of N−H···H hydrogen bonds in the conjugate acid with angles that are significantly wider in **10H**$^+$ (158.4°, 151.0°, and 145.1°) than in **8H**$^+$. This results in a much larger PA for **10** over **8**, by 11.9 kcal mol^{-1}. In view of the methyl effect noted above, methyl substitution onto the amino groups of **10** should increase its PA. Monomethylation of the aromatic amines of **10** (giving **11**) increases the PA by 10.9 kcal mol^{-1}, and permethylation of the terminal amines (**12**) results in a further increase in the PA of 3.8 kcal mol^{-1}. The PA of **12** is 13.4 kcal mol^{-1} larger than that of DMAN **1**.

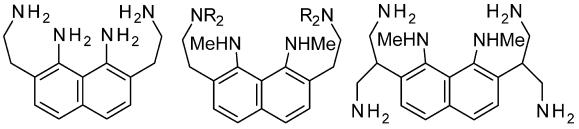

As shown in Figure 2, **11H**$^+$ is stabilized by three intramolecular hydrogen bonds, two in the first layer and one in the second layer. The addition of an aminomethyl group to each side chain creates **13**, a compound whose conjugate acid can be stabilized by five intramolecular hydrogen bonds. The optimized structure of **13H**$^+$, shown in Figure 2, indicates the two first-layer, two second-layer, and one third-layer hydrogen bonds. The addition of these two remote hydrogen bonds makes the PA of **13** 4.9 kcal mol^{-1} greater than that of **11**. **13** is the most basic of the linear acenes discussed here, though methylation of the terminal amine groups would likely increase the PA further.

Cyclohexane and Decalin Bases. The cyclohexane scaffold affords some opportunities to place amino groups in positions to participate in hydrogen-bonding networks. The reference for this scaffold is cyclohexanamine (**14**), whose computed PA (224.6 kcal mol^{-1}) overestimates the experimental value[22] by 1.3 kcal mol^{-1}.

dx.doi.org/10.1021/jo4018974 | J. Org. Chem. 2013, 78, 10909−10916

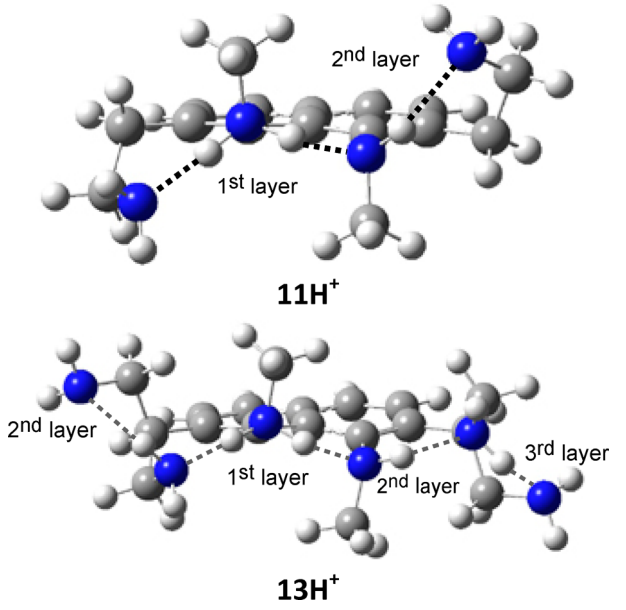

Figure 2. ωB97X-D/6-311+G(2d,p)-optimized geometries of **11H**$^+$ and **13H**$^+$.

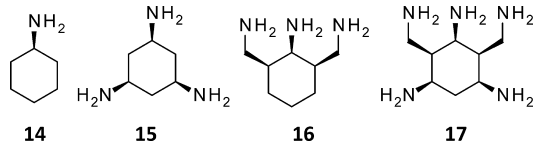

Placing amino groups at the 3 and 5 positions of **14** provides an opportunity to stabilize the ammonium through one or perhaps two first-layer hydrogen bonds. In order to do this, the amino groups must all be *cis*, as in **15**. The optimized geometry of **15** places the three amino groups into equatorial positions (Figure 3), but the optimized structure of the conjugate acid has the substituents in the axial position (necessitating a ring flip) with one intramolecular hydrogen bond (**15H**$^+$**a**). The conformation that allows for two intramolecular hydrogen bonds requires the quaternary amine−C_1 bond to be eclipsed (**15H**$^+$**b**); this conformation is a transition state separating mirror images of **15H**$^+$**a**. However, when zero-point vibrational energy is included, **15H**$^+$**b** is slightly lower in enthalpy than **15H**$^+$**a**. Thus, there is essentially free rotation about the ammonium bond in **15H**$^+$. The intramolecular hydrogen bonding in **15H**$^+$ dramatically stabilizes this cation over **14H**$^+$ and makes **15** a much more powerful base: its PA is 17.6 kcal mol^{-1} greater than that of **14** (Table 3).

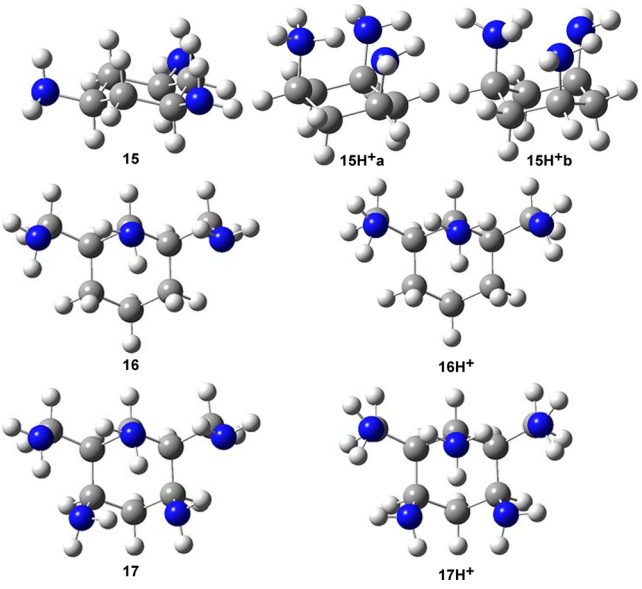

Figure 3. ωB97X-D/6-311+G(2d,p)-optimized geometries of **15**−**17** and their conjugate acids.

Table 3. ωB97X-D/6-311+G(2d,p)-Computed Proton Affinities (kcal mol^{-1}) of 14−17 and PAs Relative to That of 1

compound	PA	rel. PA
1	247.7	0.0
14	224.6	−23.1
15	242.2	−5.5
16	249.7	2.0
17	253.4	5.7

The stabilization of the conjugate acid of **16** comes about through first-layer hydrogen bonding whereby the two adjacent aminomethyl groups act as hydrogen-bond acceptors. In both the free base and the conjugate acid, the aminomethyl groups are in the equatorial position while the amino group is in the axial position. **16H**$^+$ is stabilized by two intramolecular hydrogen bonds. This in fact makes **16** a superbase, with a computed PA that is 2 kcal mol^{-1} greater than that of DMAN (Table 3).

Combining the substituents of **15** and **16** gives **17**. The conjugate acid **17H**$^+$ has intramolecular hydrogen bonds between the ammonium and each of the neighboring aminomethyl groups (as in **16H**$^+$). The two remote amino groups are involved in a bifurcated hydrogen bond to the third proton on the ammonium group (see Figure 3). This bifurcated hydrogen bond affords appreciable further stabilization, as the PA of **17** is 3.7 kcal mol^{-1} greater than the PA of **16**, or 5.7 kcal mol^{-1} greater than the PA of DMAN.

While methylation of the amino groups led to substantial increases of the PAs of the linear acene bases, methylation is unlikely to be helpful in making **17** into a stronger base. Methylation cannot occur at the central nitrogen that becomes the ammonium because all three protons are needed here to act as the donor hydrogens in the three intramolecular hydrogen bonds. Permethylation of the terminal amines would lead to significant steric repulsions that would destabilize the conjugate acid.

trans-Decalin offers a few interesting advantages over cyclohexane as a scaffold for a superbase. The *trans* ring fusion locks the ring conformation. This prescribes a set of fixed axial and equatorial positions where the amines can be placed to construct a fixed hydrogen-bonding network. Our starting base is decalin-4a-amine **18**, whose calculated PA is 230.3 kcal mol^{-1}. Monomethyl substitution on the nitrogen to give **19** increases the PA by 5.8 kcal mol^{-1} (Table 4), as expected for moving from a primary to a secondary amine.

Substituting amino groups onto both β-carbons in the axial positions (**20** and **21**) affords the opportunity to stabilize the conjugate acid through two first-layer hydrogen bonds. This is in fact observed in the optimized structures of **20H**$^+$ and **21H**$^+$, shown in Figure 4. These two intramolecular hydrogen bonds increase the PA of **20** over **18** by 19.5 kcal mol^{-1} and that of **21**

dx.doi.org/10.1021/jo4018974 | J. Org. Chem. 2013, 78, 10909−10916

Table 4. ωB97X-D/6-311+G(2d,p)-Computed Proton Affinities (kcal mol^{-1}) of 18−25 and PAs Relative to That of 1

compound	PA	rel. PA
1	247.7	0.0
18	230.3	−17.4
19	236.1	−11.6
20	249.8	2.1
21	253.1	5.4
22	257.4	9.7
23	261.0	13.3
24	266.9	19.2
25	268.8	21.1

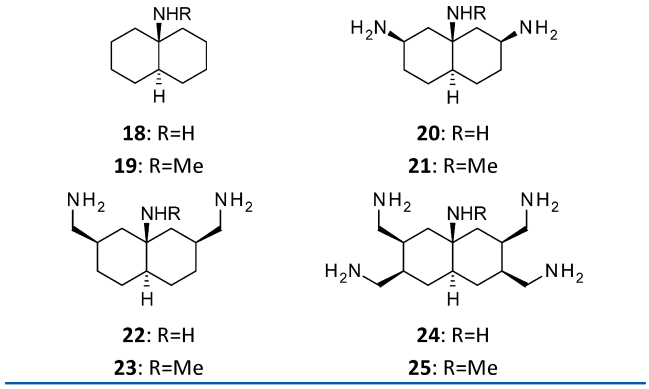

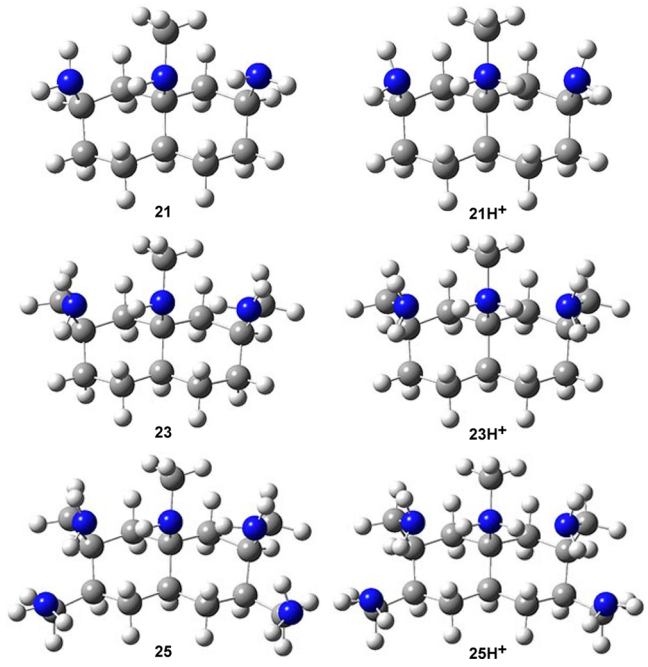

Figure 4. ωB97X-D/6-311+G(2d,p)-optimized geometries of **21**, **23**, and **25** and their conjugate acids.

over **19** by 17.0 kcal mol^{-1} (Table 4). Since the cationic charge in **19** is stabilized by the methyl group relative to the cation in **18**, there is less positive charge on the amino hydrogen in the former, so the net effect of the first-layer hydrogen bonds is less dramatic in **21** than in **20**. Both **20** and **21** are stronger bases than DMAN.

The N−H···N angles in both **20H**$^+$ and **21H**$^+$ are far from ideal (132.1° and 129.5, respectively). In addition, the N···H distances are rather long (1.937 Å in **20H**$^+$ and 2.002 Å in **21H**$^+$). As we saw in the linear acenes, moving the hydrogen-bond acceptor from a 1,3- to a 1,4-relationship can allow for a wider hydrogen-bond angle. The N−H···N angles in **22H**$^+$ are 159.2°, more than 20° wider than in **20H**$^+$. Similarly, the N−H···N angles of 155.0° in **23H**$^+$ are much wider than those in **21H**$^+$. The N···H distances have also shrunk to 1.756 Å in **22H**$^+$ and 1.798 Å in **23H**$^+$. These shortened distances and wider angles should result in stronger hydrogen bonds, stabilizing the conjugate acids and producing stronger bases. This is exactly what is observed (Figure 4 and Table 4): the PA of **22** is 257.4 kcal mol^{-1}, almost 8 kcal mol^{-1} greater than the PA of **20**, and the PA of **23** is 261.0 kcal mol^{-1}, nearly 7 kcal mol^{-1} greater than the PA of **21**.

To implement second-layer hydrogen bonding, we further substituted the decalin scaffold with additional aminomethyl groups to make **24** and **25**. The optimized structures of their conjugate acids clearly show second-layer hydrogen bonding, as seen in the structure of **25H**$^+$ presented in Figure 4. The two second-layer hydrogen bonds also result in much higher PAs: the PA of **24** is 12.5 kcal mol^{-1} greater than the PA of **22**, while the PA of **25** is 7.8 kcal mol^{-1} greater than the PA of **23**. **25** is very basic; its PA of 268.8 kcal mol^{-1} is 21.1 kcal mol^{-1} greater than that of DMAN.

Triptycene and Adamantane Bases. A quaternary ammonium cation can potentially be the donor of three hydrogens, making three intramolecular hydrogen bonds. In order to maximize the stabilization afforded by these hydrogen bonds, the conjugate acid should possess a C_3 symmetry axis. We explore here two variations on this theme: bases with a triptycene scaffold and bases with an adamantane scaffold.

9-Aminotriptycene (**26**) is a known compound,[31] though its basicity has not been explored. Its computed PA is 214.8 kcal mol^{-1}. Adding three amino groups to **26** in a 1,3-relationship creates the base **27**. Each amino group can act as the acceptor of a hydrogen bond in **27H**$^+$, as seen in the optimized structure shown in Figure 5. This structure exhibits an eclipsed

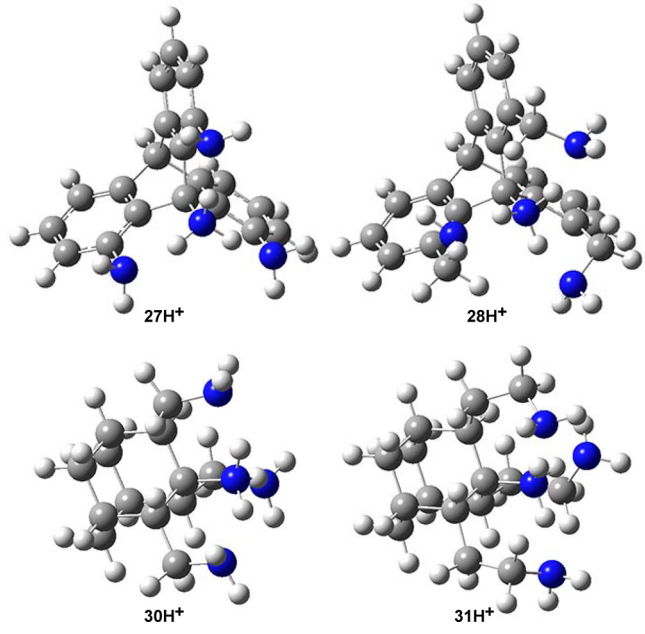

Figure 5. ωB97X-D/6-311+G(2d,p)-optimized geometries of **27H**$^+$, **28H**$^+$, **30H**$^+$, and **31H**$^+$.

dx.doi.org/10.1021/jo4018974 | J. Org. Chem. 2013, 78, 10909−10916

conformation along central the C−N bond in order to maximize the hydrogen bonding to the remote amines. The PA of **27** is 248.5 kcal mol^{-1}, almost 44 kcal mol^{-1} larger than the PA of **26** (Table 5). This dramatic increase in PA is due to the three strong intramolecular hydrogen bonds that stabilize **27H**$^+$.

Table 5. ωB97X-D/6-311+G(2d,p)-Computed Proton Affinities (kcal mol^{-1}) of 26−28 and PAs Relative to That of 1

compound	PA	rel. PA
1	247.7	0.0
26	214.8	−32.9
27	248.5	0.8
28	261.5	13.8
29	228.4	−19.3
30	265.8	18.1
31	269.5	21.8

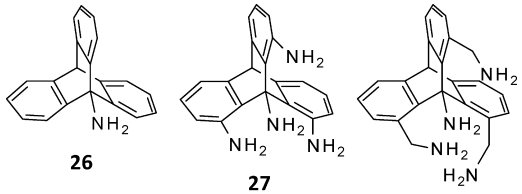

26 **27** **28**

The strong hydrogen bonds in **27H**$^+$ are reflected in their geometric parameters: the N···H distance is short (1.745 Å), and the N−H···N angle is 151.8°. Replacing the amino groups with aminomethyl groups, as we have done above, gives **28**, with the hope for hydrogen-bonding angles that are even wider than in **27H**$^+$. The geometry of **28H**$^+$, shown in Figure 5, does have somewhat better hydrogen-bond parameters, with N−H···H angles of 155.6° and N···H distances of 1.743 Å. This results in an even more basic compound: the PA value for **28** is 13 kcal mol^{-1} greater than that for **27**. **28** is a superbase, with a PA almost 14 kcal mol^{-1} larger than the PA of DMAN.

The computed PA of adamantan-1-amine (**29**) is 228.4 kcal mol^{-1}, overestimating the experimental gas-phase value[22] by about 1.6 kcal mol^{-1}. Placing aminomethyl groups at the 2, 8, and 9 positions (**30**) creates the opportunity for three intramolecular hydrogen bonds to stabilize its conjugate acid. The geometry of **30H**$^+$, shown in Figure 5, does possess three first-layer hydrogen bonds. These hydrogen bonds are slightly longer than ideal (1.819 Å), and the N−H···H angles are only 149.5°. Nonetheless, the PA of 265.8 kcal mol^{-1} for **30** is very large, 37.4 kcal mol^{-1} greater than the PA of **29**.

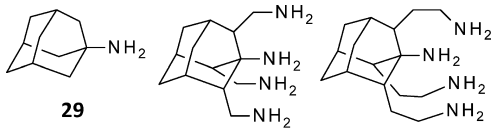

29 **30** **31**

Extending the substituent chains by one carbon makes **31**. The structure of its conjugate acid **31H**$^+$, drawn in Figure 5, clearly exhibits three intramolecular hydrogen bonds. These hydrogen bonds are shorter (1.774 Å) and have more linear N−H···H angles (161.2°) than in **30H**$^+$. In addition, the conformation about the central N−C bond is nearly ideally staggered in **31H**$^+$, while it is close to eclipsed in **30H**$^+$. Consequently, the PA of **31** is very large: 269.5 kcal mol^{-1}. The PA of **31** is the largest of all of the compounds we present here; it is 21.8 kcal mol^{-1} greater than the PA of DMAN.

Cyclophane Bases. The last scaffold explored here is [2.2]paracyclophane. Diaminoparacyclophane **32** has been prepared,[32] but its properties as a base have not been explored. The two proximal amino groups can form an intramolecular hydrogen bond to stabilize the conjugate acid, just as in DMAN. However, the distances between the two nitrogen atoms in **32** and **33** (the permethylated analogue) are long: 3.156 Å in **32** and 3.413 Å in **33**. These distances are much longer than the N···N distance of 2.798 Å in DMAN. This implies less destabilization (due to lone pair−lone pair repulsion) of the cyclophane bases relative to that of DMAN, so these bases may be weaker than DMAN.

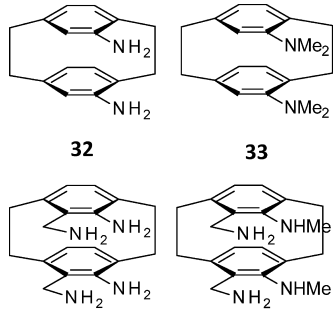

32 **33** **34** **35**

The structures of the conjugate acids of **32** and **33** are shown in Figure 6. The N···N distance does contract significantly from

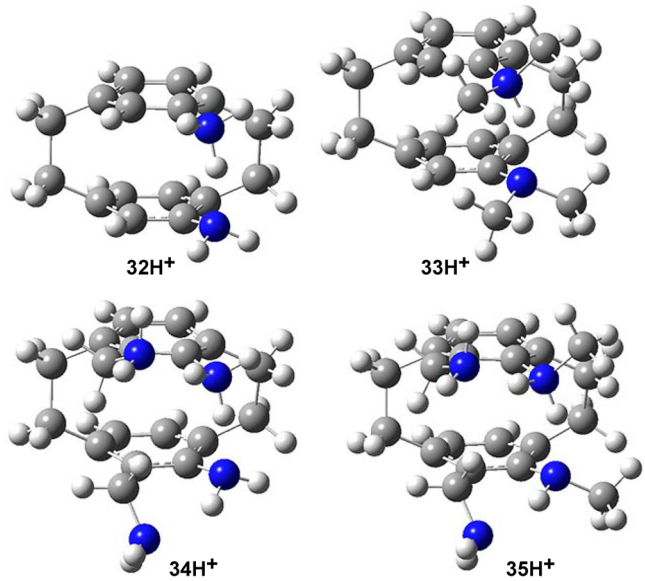

Figure 6. ωB97X-D/6-311+G(2d,p)-optimized geometries of **32H**$^+$, **33H**$^+$, **34H**$^+$, and **35H**$^+$.

that in the free base, reflecting the intramolecular hydrogen bond. While methylation does increase the basicity of **33** over that of **32**, the PA of **33** is still only 240.5 kcal mol^{-1} (Table 6), 7.5 kcal mol^{-1} less than that of DMAN.

Addition of aminomethyl groups *ortho* to each amine creates **34**. This base possesses the opportunity for a second first-layer hydrogen bond and one second-layer hydrogen bond. This is

dx.doi.org/10.1021/jo4018974 | J. Org. Chem. 2013, 78, 10909−10916

Table 6. ωB97X-D/6-311+G(2d,p)-Computed Proton Affinities (kcal mol^{-1}) of 32−34 and PAs Relative to That of 1

compound	PA	rel. PA
1	247.7	0.0
32	233.3	−14.4
33	240.5	−7.2
34	246.8	−0.9
35	252.4	4.7

evident in the optimized structure of **34H**$^+$, shown in Figure 6. These additional hydrogen bonds stabilize the conjugate acid, thus increasing the basicity of **34** over that of **32**. Nonetheless, the PA of 246.8 kcal mol^{-1} for **34** is still less than that of DMAN. Monomethylation of each of the aromatic amine groups of **34** should increase the PA to a value somewhat greater than that of DMAN. The PA of **35** was computed to be 252.4 kcal mol^{-1}, making it a superbase, but only marginally superior to DMAN. It is clear that the cyclophane scaffold is inferior to the other options examined here for creating superbases.

Solvent Effects and Entropy. The computations reported here are for the gas-phase proton affinity. We previously examined the linear acene bases in both the gas and solution phases.[21] The solution phase was modeled using a polarizable conductor model (CPCM) for cyclohexane and THF at the M06-2X/6-31+G(d) level. The inclusion of solvent made one important change: the range of the PAs relative to the PA of **1** was reduced in cyclohexane and reduced further in THF. For example, while the PA of **13** is 14.5 kcal mol^{-1} greater than that of **1** in the gas phase, it is only 10.7 kcal mol^{-1} greater in cyclohexane and 6.8 kcal mol^{-1} greater in THF.

This compression can be understood in terms of the conjugate acid. The bases examined in this study were chosen principally for their ability to stabilize the conjugate acid by delocalizing the positive charge off of a single amine center. In a solvent, even a nonpolar one like cyclohexane, the dielectric field of the solvent will aid in stabilizing any charge buildup. This stabilizing effect in the solvent will mitigate to some extent the energetic advantages afforded by the first- and second-layer hydrogen bonding relative to that in the gas phase.

Nonetheless, this compression of the range of the relative PAs of the acene bases has almost no effect on the rank ordering of the bases. In other words, the bases predicted to be stronger in the gas phase remain the stronger bases in solution. For this reason, we did not perform a solvent study for the other superbases reported here. The strongest bases we have identified in the gas phase are very likely to be strong bases in solution as well.

Another potential concern with the proposed superbases is how entropy might affect their strength. For example, the proposed superbase **31** has three ethylamino chains, each of which is locked into a particular conformation in the conjugate acid. Similarly, for **25** four methylamino chains must be in a specific conformation to achieve the extensive hydrogen-bonding network. There may be an entropic price to pay for these bases to actually pick up a proton.

It should be noted that the free bases proposed here are themselves stabilized by intramolecular hydrogen bonding. For example, the lowest-energy conformation of **23** (Figure 4) possesses two intramolecular hydrogen bonds, the same number of hydrogen bonds as in its conjugate acid **23H**$^+$. Similarly, there are four intramolecular hydrogen bonds in both **25** and **25H**$^+$ (Figure 4) and three intramolecular hydrogen bonds in both **31** and **31H**$^+$. If one chooses to compute the Gibbs free energy using just the lowest-energy conformation of both base and conjugate acid, the resulting free energy for the relative proton affinity is reduced for each of the proposed superbases, but by only 1−4 kcal mol^{-1} compared with the relative enthalpy (Table 7). The base and the conjugate acid reflect similar (but not identical) entropic demands from the intramolecular hydrogen bonds.

Table 7. Enthalpies and Free Energies (kcal mol^{-1}) of Protonation for the Potential Superbases Relative to DMAN (1)[a]

compound	ΔH	ΔG
1	0.0	0.0
10	−1.3	−3.7
11	9.6	7.1
12	13.4	10.7
13	14.5	11.4
18	−17.4	−18.4
19	−11.6	−12.4
20	2.1	0.3
21	5.4	4.1
22	9.7	7.0
23	13.3	11.2
24	19.2	17.2
25	21.1	18.9
26	−32.9	−33.9
27	0.8	0.9
28	13.8	10.2
29	−19.3	−21.2
30	18.1	14.2
31	21.8	18.2
32	−14.4	−16.8
33	−7.2	−9.3
34	−0.9	−3.8
35	4.7	1.5

[a]Computed using only the lowest-energy conformer of the base and its conjugate acid.

However, the intramolecular hydrogen bonds within the bases are weaker than those within the conjugate acids, as judged by much longer distances in the former. This is as expected: the free bases are neutral, while the hydrogen bonds are strengthened by the positive charge on the ammonium group, making those hydrogen atoms much better donors. This means that the energy differences among the low-lying conformations of the bases, many of which have fewer intramolecular hydrogen bonds, will be smaller than the energy differences among the low-lying conformations of the conjugate acids. A Boltzmann distribution will properly require many more conformers of the base and will populate more heavily this broader range of conformers than in the case of the conjugate acid. This will lead to a further reduction in the relative base strength of many of the proposed bases. Proper accounting for the free energy of protonation for the bases here will require a comprehensive conformational search, including analytical frequency analysis, a substantial computational task. Suffice it to say that the trend shown in Table 7 demonstrates that the proposed compounds are stronger bases that DMAN, especially **25** and **31**.

dx.doi.org/10.1021/jo4018974 | J. Org. Chem. 2013, 78, 10909−10916

CONCLUSIONS

Superbases are neutral organic compounds whose basicities, measured in this work through their proton affinities, exceed that of DMAN (proton sponge) **1**. The principal method for developing superbases examined here is through a hydrogen-bonding network that stabilizes the conjugate acid. This network is formed of first-layer hydrogen bonds directly to the ammonium center and then second- and third-layer hydrogen bonds emanating outward.

A number of different amine scaffolds have been investigated through computational evaluation of their proton affinities. For the linear acenes, the strongest base is **13**, which has a PA of 262.2 kcal mol^{-1}, some 14 kcal mol^{-1} larger than the PA of DMAN. The conjugate acid **13H**$^+$ displays two first-layer hydrogen bonds, two second-layer hydrogen bonds, and one third-layer hydrogen bond. Of the cyclohexane and decalin scaffolds, the latter provides a conformationally fixed platform for positioning amine groups to nicely participate in hydrogen-bonding networks. The strongest base is **25**, which has a PA of 268.8 kcal mol^{-1}, about 21 kcal mol^{-1} larger than the PA of DMAN. The conjugate acid **25H**$^+$ is stabilized by two first-layer hydrogen bonds and two second-layer hydrogen bonds.

The cyclophane scaffold was explored for its potential to serve as a superbase platform. However, the inherent large distance between the two aromatic rings inevitably means that the free base itself is not destabilized in the way DMAN and related compounds are through repulsions between neighboring lone pairs. This is manifested in bases that can be strong, such as **35** with a PA 5 kcal mol^{-1} greater than that of DMAN, but other targets are much more promising.

Triptycene and adamantane provide scaffolds that allow for the arrangement of groups to form three first-layer hydrogen bonds (with structures having a C_3 rotational axis). The best triptycene structure is **28**, with a PA that is nearly 14 kcal mol^{-1} greater than the PA of DMAN. However, the strongest base that we discovered in this study is the adamantane structure **31**; its PA is 269.5 kcal mol^{-1}, which is nearly 22 kcal mol^{-1} greater than the PA of DMAN.

While the basicities of the superbases we have proposed here were evaluated using their gas-phase proton affinities, our linear acene superbase study did show that the solution-phase basicities are strongly correlated to the gas-phase PAs.[21] The top-performing superbases examined here should therefore be considered as prime targets for synthesis and application.

ASSOCIATED CONTENT

Supporting Information

Full citation for ref 30, Figures S1 and S2, and coordinates and energies for **1**−**2** and **6**−**35** and their conjugate acids. This material is available free of charge via the Internet at http://pubs.acs.org.

AUTHOR INFORMATION

Corresponding Author

*E-mail: sbachrach@trinity.edu.

Notes

The authors declare no competing financial interest.

ACKNOWLEDGMENTS

The author thanks Trinity University for the computational resources employed in this study.

REFERENCES

(1) Alder, R. W.; Bowman, P. S.; Steele, W. R. S.; Winterman, D. P. *Chem. Commun.* **1968**, 723−724.
(2) Schwesinger, R.; Mißfeldt, M.; Peters, K.; von Schnering, H. G. *Angew. Chem., Int. Ed. Engl.* **1987**, *26*, 1165−1167.
(3) Zirnstein, M. A.; Staab, H. A. *Angew. Chem., Int. Ed. Engl.* **1987**, *26*, 460−462.
(4) Estrada, E.; Simón-Manso, Y. *Angew. Chem., Int. Ed.* **2006**, *45*, 1719−1721.
(5) Singh, A.; Ganguly, B. *Eur. J. Org. Chem.* **2007**, 420−422.
(6) Bühl, M. *Chem.—Eur. J.* **2011**, *17*, 3575−3578.
(7) Schwesinger, R.; Schlemper, H. *Angew. Chem., Int. Ed. Engl.* **1987**, *26*, 1167−1169.
(8) Schwesinger, R.; Schlemper, H.; Hasenfratz, C.; Willaredt, J.; Dambacher, T.; Breuer, T.; Ottaway, C.; Fletschinger, M.; Boele, J.; Fritz, M.; Putzas, D.; Rotter, H. W.; Bordwell, F. G.; Satish, A. V.; Yi, G. Z.; Peters, E.-H.; Peters, K.; von Schnering, H. G.; Walz, L. *Liebigs Ann.* **1996**, 1055−1081.
(9) Raab, V.; Gauchenova, E.; Merkoulov, A.; Harms, K.; Sundermeyer, J.; Kovacevic, B.; Maksic, Z. B. *J. Am. Chem. Soc.* **2005**, *127*, 15738−15743.
(10) Maksić, Z. B.; Kovačević, B. *J. Org. Chem.* **2000**, *65*, 3303−3309.
(11) Kovačević, B.; Glasovac, Z.; Maksić, Z. B. *J. Phys. Org. Chem.* **2002**, *15*, 765−774.
(12) Barić, D.; Dragičević, I.; Kovačević, B. *J. Org. Chem.* **2013**, *78*, 4075−4082.
(13) Kovačević, B.; Despotović, I.; Maksić, Z. B. *Tetrahedron Lett.* **2007**, *48*, 261−264.
(14) Despotović, I.; Kovačević, B.; Maksić, Z. B. *Org. Lett.* **2007**, *9*, 4709−4712.
(15) Maksić, Z. B.; Kovačević, B.; Vianello, R. *Chem. Rev.* **2012**, *112*, 5240−5270.
(16) Bachrach, S. M.; Wilbanks, C. C. *J. Org. Chem.* **2010**, *75*, 2651−2660.
(17) Tian, Z.; Fattahi, A.; Lis, L.; Kass, S. R. *Croat. Chem. Acta* **2009**, *82*, 41−45.
(18) Shokri, A.; Schmidt, J.; Wang, X.-B.; Kass, S. R. *J. Am. Chem. Soc.* **2012**, *134*, 2094−2099.
(19) Shokri, A.; Abedin, A.; Fattahi, A.; Kass, S. R. *J. Am. Chem. Soc.* **2012**, *134*, 10646−10650.
(20) Shokri, A.; Wang, X.-B.; Kass, S. R. *J. Am. Chem. Soc.* **2013**, *135*, 9525−9530.
(21) Bachrach, S. M. *Org. Lett.* **2012**, *14*, 5598−5601.
(22) *NIST Chemistry WebBook*; Linstrom, P. J., Mallard, W. G., Eds.; NIST Standard Reference Database No. 69; National Institute of Standards and Technology: Gaithersburg, MD, 2009; http://webbook.nist.gov.
(23) (a) Becke, A. D. *J. Chem. Phys.* **1993**, *98*, 5648−5650. (b) Lee, C.; Yang, W.; Parr, R. G. *Phys. Rev. B* **1988**, *37*, 785−789. (c) Vosko, S. H.; Wilk, L.; Nusair, M. *Can. J. Phys.* **1980**, *58*, 1200−1211. (d) Stephens, P. J.; Devlin, F. J.; Chabalowski, C. F.; Frisch, M. J. *J. Phys. Chem.* **1994**, *98*, 11623−11627.
(24) Zhao, Y.; Schultz, N. E.; Truhlar, D. G. *J. Chem. Theory Comput.* **2006**, *2*, 364−382.
(25) Chai, J.-D.; Head-Gordon, M. *Phys. Chem. Chem. Phys.* **2008**, *10*, 6615−6620.
(26) Bachrach, S. M. *Annu. Rep. Prog. Chem., Sect. B: Org. Chem.* **2008**, *104*, 394−426.
(27) Pieniazek, S. N.; Clemente, F. R.; Houk, K. N. *Angew. Chem., Int. Ed.* **2008**, *47*, 7746−7749.
(28) Grimme, S. *Org. Lett.* **2010**, *12*, 4670−4673.
(29) Krieg, H.; Grimme, S. *Mol. Phys.* **2010**, *108*, 2655−2666.
(30) Frisch, M. J.; et al. *Gaussian 09*, revision A.02; Gaussian, Inc.: Wallingford, CT, 2009.
(31) Imashiro, F.; Hirayama, K.; Terao, T.; Saika, A. *J. Am. Chem. Soc.* **1987**, *109*, 729−733.
(32) Shaieb, K. E.; Narayanan, V.; Hopf, H.; Dix, I.; Fischer, A.; Jones, P. G.; Ernst, L.; Ibrom, K. *Eur. J. Org. Chem.* **2003**, 567−577.